

ORIGINAL RESEARCH

Vibration signal diagnosis and conditional health monitoring of motor used in biomedical applications using Internet of Things environment

Dong Wang¹ | Lihua Dai¹ | Xiaojun Zhang² | Shabnam Sayyad³ | R. Sugumar⁴ |
Khushmeet Kumar⁵ | Evans Asenso⁶ 

¹Suzhou Vocational Institute of Industrial Technology, Suzhou, Jiangsu, China

²Soochow University, Suzhou, Jiangsu, China

³Department of Computer Engineering, AISSMS College of Engineering, Pune, India

⁴Department of Computer Science Engineering, Saveetha School of Engineering, Saveetha Institute of Medical and Technical Sciences, Thandalam, Chennai, India

⁵Department of Mechanical Engineering, Baddi University of Emerging Sciences and Technology (BUEST), Baddi, Himachal Pradesh, India

⁶Department of Agricultural Engineering, University of Ghana, Ghana

Correspondence

Evans Asenso, Department of Agricultural Engineering, University of Ghana, Ghana.
Email: easenso@ug.edu.gh

Abstract

Vibration, especially basic vibration, may cause loose contacts, open circuits, or other contact problems, which account for a large proportion of system failure causes. Due to the complexity of the chassis structure used in the biomedical motors, the vibration analysis of a single component cannot solve the vibration problems encountered in the work of the system. Therefore, it is necessary to use system simulation and experiments to monitor and enhance the health of the structure. Finite element method is used to carry out the dynamic analysis from the component to the system, and calculate the natural frequency, modal shape and harmonic response. Then, the effectiveness and accuracy of the analysis results are verified by experiments through simulation and experiments. The results show that the measures taken have effectively reduced the vibration of the chassis equipment and improved its safety for better health safety of patients. There is just a 2% variation between the natural frequencies acquired from the experiment and the simulation computation. In terms of natural frequency, the first 6-order natural frequencies all have errors of less than 10%, and the natural frequency error is comparable to that of fireproof board.

1 | INTRODUCTION

With the rapid development of the Internet of Things (IoT), its application has been involved in many fields, such as intelligent control, structural health monitoring, biomedical application. IoT applications in health and biomedicine are key areas of study. Some of the IoT applications include hospital management systems, remote patient monitoring, medical waste management, robotic nursing assistants, cancer detection via body scanning, Parkinson patient monitoring, dementia patient monitoring via GPS smart soles, depression monitoring via smartwatches, glucose monitoring, efficient drug management, and hand hygiene monitoring. In Biomedical application motors are been used for different purpose such as:

- For Mobility: Different motors with help of gear system is used in wheelchair to make the patients enjoy their freedom.

- Used in Medical pumping: In Biomedical application like computed tomography (CT) scanner, Dialysis, continuous positive airway pressure (CPAC) machines and many more uses different motors for cooling the medical operative machine, help meter fluids for proper indication, help transfer of gases inside the medical equipment's.
- Used in Robotic Operations and surgery: Now a days doctors are assist with robotic arms and devices to take part in surgical operation. These robotic arms and devices must be accurate and reliable
- Motor powered prosthetics: To eliminate the disability of any human being artificial limbs play a vital role in this 21st century. These artificial limbs are powered with motors for their operations.

From the above discussion it is clear that there is requirement of better conditional health monitoring of motor such

This is an open access article under the terms of the [Creative Commons Attribution](https://creativecommons.org/licenses/by/4.0/) License, which permits use, distribution and reproduction in any medium, provided the original work is properly cited.

© 2022 The Authors. *The Journal of Engineering* published by John Wiley & Sons Ltd on behalf of The Institution of Engineering and Technology.

that secondary damage which include human life can be saved.

As a basic part of the Internet of Things system, the chassis equipment must have the ability to route billions of data packets within a few seconds. The network quality that connects these online devices and affects the communication speed determines the development of the Internet of Things. In order to improve communication speed and network quality, chassis equipment must usually be placed on site, which means that they will be exposed to unprecedented conditions such as extreme temperature, humidity, corrosive smoke, and mechanical vibration [1]. Because of the Internet of Things, wireless sensor networks (WSNs), which are made up of several sensors, are commonly used in monitoring essential equipment. The massive amount of data acquired by sensors, which has profited from the advancement of data mining technologies, simplifies condition monitoring and issue identification [2, 3]. Various devices are used now days for vibration measurements. Accelerometers are used in a wide range of applications, such as condition monitoring, activity recognition, and vehicle monitoring. Accelerometers are also used to track motion in most handheld smart devices, such as Smartphone. The physical limitations of such devices have spurred the demand for precise, affordable, tiny, and power-efficient accelerometers [4, 5]. Among these environmental factors, vibration, especially basic vibration, may cause loose contacts, open circuits, or other contact problems, which account for a large proportion of system failure causes. Therefore, system-level simulation and experiments are needed to monitor and enhance the structural health of IoT chassis equipment. The contribution of the current study are given below:

- The authors of the current study used system simulation and experimentation to improve the chassis equipment's structural strength.
- The dynamic analysis from the component to the system is performed using the finite element method.
- The natural frequency, modal shape, and harmonic response of a specific Internet of Things chassis equipment are calculated.
- Experiments are used to validate the effectiveness and correctness of the analytical results.
- The weak points of the entire system are identified through simulation and experiment, and then recommended solutions to enhance the structure and reduce vibration are tested in both simulation and experiment.

1.1 | Finite element analysis

The finite element simulation for this IoT chassis equipment is implemented in ANSYS Workbench. The size of the chassis is 450 mm × 450 mm × 50 mm, as shown in Figure 1, which is mainly composed of six parts: the bottom plate, the skeleton, the left and right circuit boards, the circuit board bracket, the power module and the upper case [6]. At the same time, set the circuit board support to be translucent. A large T-shaped

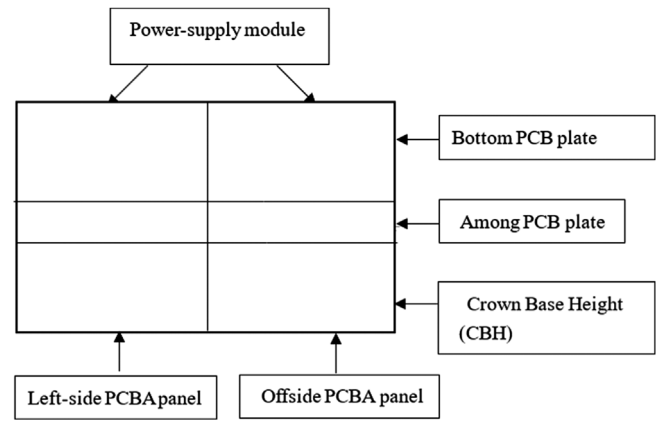


FIGURE 1 Chassis geometric model diagram

printed circuit board assembly (PCBA) board is fixed on the bottom plate, which is shown in dark yellow in the Figure. The left and right circuit boards are connected to the middle frame through the circuit board bracket, and each circuit board is composed of the PCBA board and the fireproof board on the back. The PCBA board is displayed in green. When measuring the vibration of the circuit board, the main measurement is the PCBA board [7]. PCBs are circuit boards that link electronic components together. They're a crucial component of the electronics we use in our daily lives, and they're used in a variety of sectors. They're constructed of a non-conductive substance with lines, pads, and other features carved from copper sheets to link the electronic components of a device electrically. Some PCBs additionally include components such as capacitors and resistors put on them. When designing printed circuit boards (PCBs), keep the following major cause of electronic failure in mind: temperature cycling, tremor, mechanical stress and drop. A variety of testing methods may be used to determine how and why electronics fail, but PCB modelling and simulation is a significantly quicker and cheaper approach [8, 9]. As the experimental measurement requires that the laser beam can directly reach the point to be measured, while the left and right PCBA boards are blocked by the upper case and the circuit board bracket, the material corresponding to the two large square holes is removed from the upper case of the case. The product's geometrical and technical representations are contained in the design model. It provides the geometric and technological assistance that analysis requires. Constraints on design parameters are also part of the design model. They're an operating version of the criteria in the requirements list, and they're a first step in defining the analysis aim. When a new chassis is designed, the shell model supplied is used to compute global stiffness (validation of the first need to enhance rigidity under torsion and bending loads) and maximum stresses in the structure (validation of the design in terms of resistance). The chassis model which is connected with various parts as shown in Figure 1. The bottom plate, the left and right side panel, the circuit board bracket, the power module and the upper case and the Crown Base Height (CBH). On the bottom plate, which is depicted in dark yellow in the Figure, a sizable PCBA board in the shape of a

TABLE 1 Initial material parameter settings of chassis components

Chassis components	Density/ (kg m^3)	Elastic modulus/ GPa	Poisson's ratio
Bottom plate	2000	26	0.28
Bracket	2770	61	0.33
PCBA board	3300	25	0.28
Skeleton	7850	200	0.3
The upper case	7850	200	0.3

T is fixed. Each circuit board is made up of a PCBA board and a fireproof board on the back, and the left and right circuit boards are joined to the main frame via the circuit board bracket. Green text is used to display the PCBA board. The PCBA board is the primary measurement for assessing the vibration of the circuit board.

1.2 | Parameter index

In the calculation, the initial material parameter settings of each component are shown in Table 1. Since each PCBA board contains parts such as chips, heat sinks, connectors, and fireproof steel plates, and is not composed of a single material, its actual calculation parameters need to be adjusted accordingly after comparing with the experimental results [10–12]. Sometimes in circumstances, the reaction of the shock and/or vibration environment will play a significant part in the overall damage. These dynamic effects can cause the structure to resist substantial amplitudes and/or acceleration levels, whether generated by the environment, manufacture, shipping, handling, operation, or any other source [13, 14]. As a result, the issue of shielding PCBs against the effects of acute vibration should be addressed. To begin with, it is critical to fast and accurately model the systems in order to acquire a good vibration reliability estimate [15, 16]. The PCBA board is fixed on the skeleton by screws and connectors. In order to facilitate calculations, detailed features such as screws and pins are removed from the finite element model, and the surfaces of the two components at the connection of the corresponding position are bound together in ANSYS as a simplified contact condition.

After setting each parameter, modal analysis and calculation are performed, and the first 60-order modes including many local modes are extracted by the block Lanczos method [17–19]. After obtaining the natural frequency and mode shape of the system, in order to determine the deformation of each part of the structure under different frequencies of simple harmonic loads, a harmonic response analysis is required. The results of the analysis can be used to predict the continuous dynamic characteristics of the structure and help verify whether the system can overcome harmful factors such as resonance, fatigue and other forced vibrations. The harmonic response analysis can use the complete method, the reduction method and the modal superposition method. Here, the modal superposition

method is used to solve the problem. The scanning frequency is 30–300 Hz. A basic acceleration of $0.5 \times g$ is applied to the whole model to incent it. The incentive direction is vertical downward, perpendicular to the horizontal chassis, and the incentive position is the whole chassis. Because the intensity of different order vibrations in the system is different, with the change of frequency, some contacts in the system are strong and weak, resulting in the change of damping. Therefore, setting a single constant damping in the model is inconsistent with the actual situation [20]. In order to better simulate the experimental results, the finite element model uses the assumption of modal damping, and sets different modal damping ratios according to different modals. Use the MDAMP command in ANSYS to input the modal damping ratio into the analysis model. The damping ratios of the first five-order modes are 0.0035, 0.1, 0.4, 0.04, and 0.006, respectively. The value of the damping ratio of each mode is determined after the comparison and adjustment of simulation and experimental results. The vibration properties of the chassis assembly are investigated in this study, as well as damping adjustment. However, because of the huge number of internal elements of the chassis and the intricate contact circumstances, doing a direct finite element analysis of the assembly is not only difficult, but also time consuming. Find the source and transmission channel of severe vibration in the chassis structure using harmonic response analysis, then implement suitable optimization steps to minimise vibration. Finally, perform simulation analysis to validate the vibration reduction measures.

2 | LITERATURE REVIEW

At present, many results have been achieved in the vibration analysis of the internal components of the chassis in many aspects such as soldering points, connectors, and PCBA. For example, Che et al. conducted vibration fatigue experiments and analysis on flip chip solder joints, and developed a quasi-static finite element analysis method to study the stress–strain behaviour in the prediction of the solder joint vibration fatigue life, as shown in Figure 2 [21]. Bo Zhang et al. constructed a finite element model for standard PCBA boards assembled in three chip sizes, and verified the analysis results through modal tests [22]. It should be noted that the finite element model discussed in these studies is mainly a part of the entire system, while as a complex of many components, the characteristics of a system affect each other, and even the characteristics of the joint surface between components will be superimposed on the system characteristics [23–26]. Therefore, it is still a challenging task to analyze the vibration characteristics of chassis equipment at the system level. Conle and Mousseau [27] published an analytical assessment of the fatigue life of vehicle chassis components based on automotive proving ground load history data and current computational breakthroughs. Sane et al. [28] used an iterative technique to do stress analysis on a light commercial vehicle chassis in order to reduce stress levels at crucial areas. Guo and Chen [29] investigate the dynamic and modal analysis of a space chassis (complex 3D chassis) and use the principle of superposition to analyse transient response. In order to capture

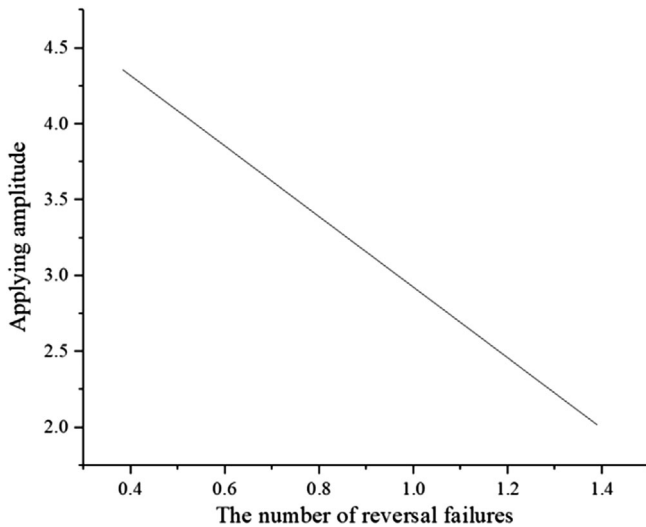


FIGURE 2 Fatigue life curve

these vibration-coupled difficulties, engine mounting systems with flexible foundations must be modelled [30]. The coupling effects were shown to be significant for frequencies lower than idle speed but insignificant for frequencies greater than idle speed in prior studies. Kotari and Gopinath [31] give a study of a chassis frame for enhancing payload capacity by adding stiffener and c channel at the greatest stress zone of the chassis frame, which results in a 20% increase in payload capacity. In [32], Marzban et al. provided the most essential characteristics, such as material, thickness, form, and impact condition, and analysed them for the design and analysis of an automotive front bumper beam in order to improve crashworthiness in low-velocity impacts. Xu et al. [33] introduced a novel finite element solver. The solid-shell element model is competitive enough in the simulation of medium thick plate metal forming and spring back, according to the findings.

Internet of Things (IoT) technologies are expanding quickly across many industries, including healthcare services, and provide exciting promise in terms of technology, business, and society. The use of wearable technology and its many health monitoring applications is fuelling the growth of the Internet of Medical Things (IoMT). By identifying diseases early, the IoMT significantly contributes to lowering death rates [34]. For the treatment of patients in crises, fog computing is a developing trend in the healthcare industry. Fog computing enhances the quality of services in the heterogeneous network, which leads to better outcomes in the healthcare industry. In order to save the lives of people, it is necessary to transport vital multimedia medical data in real-time via higher-quality networks [35].

This article studies the vibration characteristics and damping optimization of the chassis assembly. However, due to the large number of internal parts of the chassis and the complex contact conditions, if the finite element analysis of the assembly is directly carried out, it is not only difficult to set the material parameters, but also easy to set the wrong contact surface parameters. Therefore, the simulation analysis of the chassis is carried out step by step in the order of parts-semi-

assembly-chassis as a whole. First, determine the parameters of the component materials through the analysis of the components. After the analysis of the components is completed, the components are gradually assembled and analyzed, and the parameters of the contact surfaces between the components are determined in turn. After the components are fully assembled and all the contact parameters are determined, the analysis model that can replace the actual chassis is obtained. Through harmonic response analysis, find out the location of severe vibration in the chassis structure, analyze the source and transmission path of vibration, take reasonable optimization measures to reduce vibration, and then conduct simulation analysis to verify the vibration reduction measures. In order to verify the finite element model analyzed above, the experiment test the natural frequency and mode shape of each component, semi-assembly and the chassis as a whole, as well as the harmonic response of the chassis, and then compare experimental results with the numerical analysis results [36–38].

During the measurement, the chassis and rigid frame are fixed on the horizontal platform, and the horizontal platform is incited with a sine frequency sweep signal with an amplitude of $0.5 \times g$. The scanning frequency range is 30–300 Hz, and the scanning rate is 1 Hz/s. It is believed that the incentives received by the chassis are consistent with those received by the platform [39–43]. Taking the two PCBA boards inside the measuring device as an example, the scanning laser vibrometer scans the 112 positions in the Figure one by one, and then calculates the natural frequency and mode shape based on the experimental results. Extract the harmonic response amplitude of the measured point and the platform measured by the reference accelerometer, and take the ratio of the two as the vibration magnification to reflect the vibration.

3 | METHOD

3.1 | Vibration response analysis method

The differential equation of motion with viscous damping and multiple degrees of freedom:

$$[M]\{X\} + [C]\{X\} + [K]\{X\} = \{F(t)\} \quad (1)$$

The modal equation is:

$$[\Phi][M][\Phi]\{\gamma\} + [\Phi][C][\Phi]\{\gamma\} + [\Phi][K][\Phi]\{\gamma\} = [\Phi]\{F(t)\} \quad (2)$$

where $[\Phi]$ is the modal matrix. According to the orthogonality principle, only the diagonal elements of the modal mass matrix and the stiffness matrix are not zero. Due to the complexity of damping, when modal changes are made to viscous damping, it cannot be made into a diagonal matrix. The approximate method of proportional damping can be adopted to diagonalize the damping matrix. In actual work, the damping matrix $[C]$ is usually not established first, but the modal damping ratio is first obtained through modal tests, and then the damping term is added to the modal equation.

The modal matrix $[\Phi]$ is composed of the main vibration shapes from low to high, which can be obtained in turn by the matrix iteration method [2]. The iteration matrix is as follows:

$$\bar{A}X = \bar{\lambda}X \quad (3)$$

where,

$$\begin{aligned} \bar{A} &= K^{-1}M \\ \bar{\lambda} &= 1/\omega^2 \end{aligned} \quad (4)$$

It can be assumed that the initial vector is X_1 , which can be expressed by superposition of main vibration modes:

$$X_1 = c_1 \Phi_1 + c_2 \Phi_2 + c_3 \Phi_3 + \dots + \quad (5)$$

where c_1 is a constant, and the two sides of the equation are multiplied by the matrix \bar{A} to get:

$$\bar{A}X = X_2 = c_1 \bar{A}\Phi_1 + c_2 \bar{A}\Phi_2 + c_3 \bar{A}\Phi_3 + \dots + \quad (6)$$

Since each vibration mode satisfies the following relationship:

$$\bar{A}\Phi_i = \frac{1}{\omega_i^2} \Phi_i \quad (7)$$

The right side of equation (6) becomes:

$$X_2 = c_1 \frac{1}{\omega_1^2} \Phi_1 + c_2 \frac{1}{\omega_2^2} \Phi_2 + c_3 \frac{1}{\omega_3^2} \Phi_3 + \dots + \quad (8)$$

After n iterations, X_n is obtained:

$$\bar{A}X_{n-1} = X_n = c_1 \frac{1}{\omega_1^{2n}} \Phi_1 + c_2 \frac{1}{\omega_2^{2n}} \Phi_2 + c_3 \frac{1}{\omega_3^{2n}} \Phi_3 + \dots + \quad (9)$$

3.2 | The differential equation of modal motion of forced motion can be expressed as

$$\begin{aligned} &[\Phi][M][\Phi]\{\gamma\} + [\Phi][C][\Phi]\{\gamma\} + [\Phi][K][\Phi]\{\gamma\} \\ &= [\Phi]\{F(t) - [\Phi_m]x_s - [\Phi_c]x_c\} \end{aligned} \quad (10)$$

where $[\Phi_m] = [M_{II}] + [\Phi_s] + [M_{is}]$ is the effective mass matrix of the forced motion degrees of freedom $[\Phi_c] = [C_{ii}][\Phi_i] + [C_s]$, is the effective damping matrix of the forced motion degrees of freedom. The above analysis is a theoretical method to solve the vibration response. Combined with the finite element method, the vibration response of a complex model can be solved. The specific method is to discretize the model by the finite element method, and obtain the mass and stiffness matrix, and then use the matrix iteration method to get the modes of each order, and then use the modal motion equation to get the

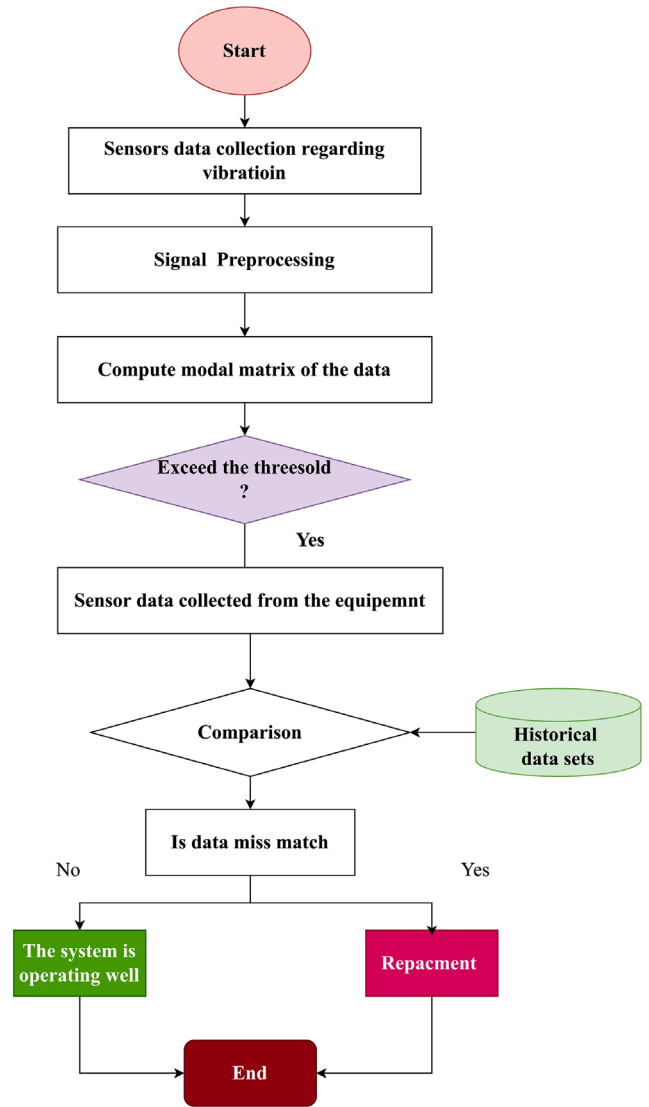


FIGURE 3 Proposed conditional monitoring of motor

model's response to the incentives. Figure 3, show the overall flowchart of the proposed system. The sensors attached with the motors collect continuous data. The sensors collect data of vibration in the chassis of the motor and send to the signal processing unit. The signal processing unit process the signal by eliminating the bad data of the system. The data must be pre-processed to eliminate detector errors before we begin the sampling procedures. The most crucial step in data processing is pre-processing. Data pre-processing procedures get the data ready for analysis. Modelling the data to derive usable data is the next step after data are gathered as an experiment's result. The data output may be excessively large, insufficiently small, or fragmented. The first step in pre-processing data is classifying it into one of these three categories and processing it accordingly. ANSYS includes functions like "resampling" and "decimate" that assist us in achieving some of the goals. For every biomedical application the vibration threshold is fixed and in case the system increases the threshold value, then the comparison with

TABLE 2 Comparison between simulation results and experimental results of natural frequency

Method	Order		
	1	2	3
Simulation results /Hz	39.613	59.12	102.45
Experimental results /Hz	39.28	58.13	104.38
Error/%	0.85	1.70	1.85

historical data sets is mandatory. If the compared data is mismatch with the predefined value means the system needs visual inspection otherwise working well. When modal modifications are made to viscous damping, it cannot be turned into a diagonal matrix due to the intricacy of damping. The particular technique is to use the finite element method to discretize the model and acquire the mass and stiffness matrix, then use the matrix iteration method to obtain the modes of each order, and then use the modal motion equation to determine the model's reaction to the incentives. The vibration response of a complicated model may be addressed using this approach in conjunction with the finite element method.

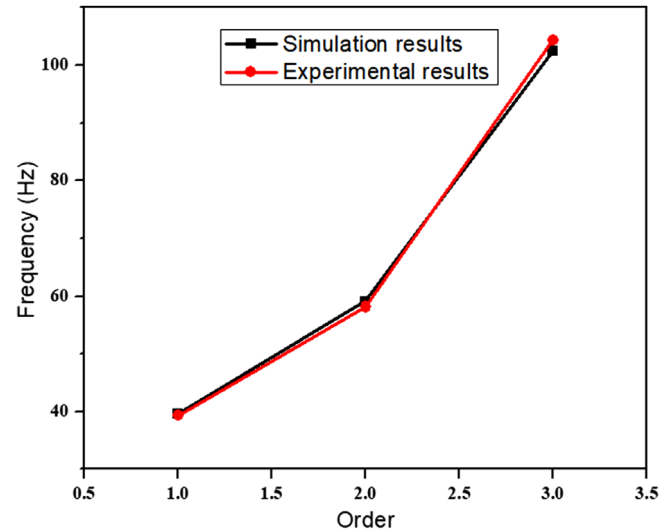
4 | RESULTS AND ANALYSIS

Here, the finite element analysis and experimental results are compared for motor conditional monitoring for biomedical application. In the entire study process, in order to determine the material parameters and the parameters between each contact surface, the results of the components, semi-assembled body and the whole chassis were compared in turn with the historical datasets. While the vibration at the connection of the PCBA board is mainly controlled during vibration reduction. Therefore, due to length and in order to highlight the focus of the study, only the vibration of the two PCBA boards in the left and right circuit boards inside the chassis are listed here. The modes of the two PCBA plates are selected and compared with the vibration amplification curve of point 111 at the end connector of PCBA plate [44, 45]. The curves of the first 3-order natural frequencies, mode shapes and vibration magnifications with local modes removed are shown in Table 2.

Table 2 and Figure 4 show that there is a fundamental correlation between the experimental results and the response magnification derived from the simulation study. Less than 2% distinguish the experimental results natural frequencies from the simulation calculation. Additionally, the modal form is essentially the same, showing that the chassis equipment finite element model choice is suitable.

4.1 | PCBA single board on the left circuit board

After parameter adjustment during the simulation, the simulation frequency of the PCBA single board on the left side circuit

**FIGURE 4** Comparison between simulation results and experimental results**TABLE 3** Comparison of simulation of PCBA single board on the left

Order	1	2	3	4	5	6
Simulation /Hz	63.823	114.04	124.56	174.01	203.9	281.11
Experiment/Hz	60	109.38	123.75	175	223.75	305.63
Error/%	6.37	4.26	0.65	0.57	8.87	8.02

TABLE 4 The simulation table of the left circuit board

Order	1	2	3	4	5	6
Simulation /Hz	83.307	145.12	181.06	222.73	278.18	315.04
Experiment/Hz	89.38	145	181.88	202.5	313.75	322.5
Error/%	6.79	0.082	0.45	9.99	11.33	2.31

board and the experimental results of the corresponding mode shape are obtained, as listed in Table 3.

From the results of simulation and experiment, in terms of natural frequency, the errors of the first 6-order natural frequencies are all within 10%, which is smaller than the error of the fire board. In terms of modal shape, except for the fourth-order mode, the rest of the rest modal matching is good.

4.2 | Left circuit board

After installing the fireproof board of the left circuit board and PCBA veneer together, experiments and simulations are carried out to compare the vibration of the front side of the PCBA single board. After parameter adjustment, the free-state simulation frequency of the circuit board and the corresponding experimental results are obtained, as listed in Table 4.

It can be seen from the table that the simulation and experimental results of each order have been determined basically, and

TABLE 5 Comparison between simulation results and experimental results of right circuit board

Order	1	2	3	4	5	6
Simulation /Hz	91.919	166.51	189.33	314.31	392.31	455.7
Experiment/Hz	91.88	161.88	182.5	315.63	345	438.13
Error/%	0.042	2.86	3.74	0.41	13.71	4.01

TABLE 6 Comparison between simulation and experimental frequency of the upper case on the chassis

Order	1	2	3	4	5	6
Simulation /Hz	23.558	40.156	45.3	59.268	83.722	87.638
Experiment/Hz	23.75	38.75	50	60.63	76.88	86.88
Error/%	0.81	3.63	9.40	2.25	8.90	0.87

the error of natural frequency is not larger than that of fireproof board. Because the material parameters increase when the single board is measured separately, it means that the contact condition definition of the circuit board on the left is basically correct.

4.3 | Right circuit board

The circuit board on the right only carries out the experiment and simulation of the combination of the fireproof board and the PCBA single board. After comparison, the free-state simulation frequency and the corresponding experimental results are obtained, as listed in Table 5.

From the results, in terms of natural frequency, results of the fifth-order natural frequency are quite different, except for that the difference between the first six results is very small. But the error of the fifth-order is within 15%, the result is acceptable. In terms of mode shape, the results of the first four-order simulation and experiment are basically consistent, and the first six-order mode shapes are relatively consistent, indicating that settings of the material parameters and contact condition definition of the right circuit board are accurate.

4.4 | The upper case

In the separate experimental analysis of the upper-case components, two large square holes were not opened, so the upper-case model obtained at this situation is a complete case. After adjusting the parameters during simulation, the simulation and corresponding experimental frequency of the upper case are obtained, as listed in Table 6.

Because the structure of the upper case is simple, it is easy to adjust the parameters during simulation. According to the results, the frequency and mode shape of the upper case on the chassis can be matched well, indicating that the simulation parameter settings are consistent with the real situation [46, 47]. It can be seen from the results that the vibrating position corre-

TABLE 7 Comparison between simulation and experimental frequency of bottom circuit board

Order	1	2	3	4	5	6
Simulation /Hz	24.547	37.594	57.45	76.484	102.2	105.06
Experiment/Hz	26.88	44.38	60.63	75	90.63	105.63
Error/%	8.68	15.29	5.24	1.98	12.77	0.54

sponding to the low-order natural frequency is the edge of the upper case, while the violent vibrating position corresponding to the high-order natural frequency is the middle part of the upper case.

4.5 | PCBA single board at the bottom

After adjusting the simulation parameters, the simulation and corresponding experimental frequency of the bottom PCBA single board are obtained, as listed in Table 7.

It can be seen from the results that because the bottom PCBA board is a thin-plate structure with a large area, its natural frequency is low. The absolute value of the simulation and experimental results of some natural frequencies is relatively small [48, 49]. However, the relative percentage is relatively large, which causes the error of some natural frequencies to exceed 10%. In terms of mode shape, the experimental and simulation results of the first six order modes are relatively consistent, and the results are generally acceptable [50, 51].

5 | CONCLUSION

This study analyses and studies the system level vibration characteristics and vibration reduction of a motor chassis Internet of Things device used for biomedical application. The natural frequency, modal shape, and harmonic response of the biomedical motor chassis equipment under the system level fundamental incentives are first computed using the finite element method to perform dynamic analysis from the component to the system. Experiments are then used to confirm the efficacy and correctness of the analytical results. The weak points of the entire system are identified through modelling and experiment, and the source and transmission path of vibration are examined. The proposed actions to reinforce the structure and vibration are confirmed in simulation and experiment. The outcomes demonstrate that the actions performed have successfully decreased the chassis equipment's vibration and enhanced its safety in biomedical applications. In future we are planned to use IoT based Wireless Sensor Network (WSN). WSN is a well-known sensing technology for data collection in intelligent monitoring and surveillance applications. Power failure or nodes being infiltrated by enemy attacks, the deployment of nodes within WSN is unavoidable. The installed node could be a malicious node that compromises and obstructs the IoT-based smart applications' ability to gather data.

AUTHOR CONTRIBUTIONS

D.W.: Conceptualization; Methodology; Writing – original draft; Writing – review and editing. L.D.: Formal analysis; Investigation; Writing – review and editing. X.Z.: Data curation; Methodology; Validation; Writing – review and editing. S.S.: Formal analysis; Methodology; Writing – original draft. R.S.: Conceptualization; Writing – original draft; Writing – review and editing. K.K.: Formal analysis; Investigation; Writing – review and editing. E.A.: Formal analysis; Methodology; Writing – review and editing

FUNDING INFORMATION

The authors received no funding for this work.

CONFLICT OF INTEREST

Authors have no conflicts of interest to disclose

DATA AVAILABILITY STATEMENT

Data can be made available from the corresponding authors on request.

ORCID

Evans Asenso  <https://orcid.org/0000-0003-3116-6356>

REFERENCES

- Zhang, Z., Chen, H., Li, D., Zhang, Z.: Stability control of the equipment recovery passage in a fully mechanized longwall mining: Case study. *Geotech. Geol. Eng.* 39(2), 799–813 (2021).
- Banaee, H., Ahmed, M., Loutfi, A.: Data mining for wearable sensors in health monitoring systems: A review of recent trends and challenges. *Sensors* 13(12), 17472–17500 (2013).
- Vyas, S., Bhargava, D., Bhola, J., Ujjan, J.A., Eswaran, S., Rahmani, A.W.: Critical retrospection of performance of emerging mobile technologies in health data management. *J. Healthcare Eng.* 2022, 8903604 (2022). <https://doi.org/10.1155/2022/8903604>.
- Iqbal, U., Mir, A.H.: Efficient and dynamic access control mechanism for secure data acquisition in IoT environment. *Int. J. Comput. Digital Syst.* 10(1), 9–28 (2021).
- Sriram, G.S.: Resolving security and data concerns in cloud computing by utilizing a decentralized cloud computing option. *Int. Res. J. Mod. Eng. Technol. Sci.* 4(1), 1269–1273 (2022)
- Guo, W., Zhu, G., Yao, B., Chen, F., Xu, X.: Study on the fire extinguishing mechanism of small size wood crib based on small sand-throwing equipment. *Case Studies Thermal Eng.* 25(6), 100942 (2021).
- Yao, B., Zhu, G., Guo, W., Chen, F., Xin, X.: Experimental study of the effectiveness of sands on extinguishing pool fires based on small sand-throwing equipment. *Case Studies Thermal Eng.* 28(8), 101408 (2021)
- Schuerink, G.A., Slomp, M., Wits, W.W., Legtenberg, R., Kappel, E.A.: Modeling printed circuit board curvature in relation to manufacturing process steps. *Procedia CIRP* 9, 55–60 (2013).
- Chan, F.T.S., Chan, H.K.: Simulation analysis of a PCB factory using factorial design - A case study. *Int. J. Adv. Manuf. Technol.* 21(7), 523–533 (2003).
- Na, K.M., Jung, H., Park, Y.: Life-cycle assessment of a railway electric power feeding cable for replacement planning: a case study of an electric railway in Korea. *J. Electr. Eng. Technol.* 16(4), 2275–2280 (2021)
- Mohseni, S., Brent, A.C., Burmester, D., Browne, W.N.: Lévy-flight moth-flame optimisation algorithm-based micro-grid equipment sizing: an integrated investment and operational planning approach. *Energy AI* 3(5), 100047 (2021).
- Chowdhury, H., Chowdhury, T., Hossain, N., Chowdhury, P., Mahlia, T.: Exergetic sustainability analysis of industrial furnace: a case study. *Environ. Sci. Pollut. Res. Int.* 28(11), 1–8 (2021).
- Guo, A., Jiang, A., Lin, J., Li, X.: Data mining algorithms for bridge health monitoring: Kohonen clustering and LSTM prediction approaches. *J. Supercomput.* 76(2), 932–947 (2019).
- Kadmin, A.F., Hamzah, R.A., Abd Manap, M.N., Hamid, M.S., Abd Gani, S.F.: Improved stereo matching algorithm based on census transform and dynamic histogram cost computation. *Int. J. Emerg. Technol. Adv. Eng.* 11(8), 48–57 (2021).
- Rashed Mohassel, R., Fung, A., Mohammadi, F., Raahemifar, K.: A survey on Advanced Metering Infrastructure. *Int. J. Electr. Power Energy Syst.* 63, 473–484 (2014)
- Su, C., Zhang, Y., Zhao, Q.: Vibration reliability sensitivity analysis of general system with correlation failure modes. *J. Mech. Sci. Technol.* 25(12), 3123–3133 (2011).
- Fee, E., Thieu, H.T.: 66. vacutainer tube alternative vaginoscopy technique in a prepubertal female: a case report. *J. Pediatr. Adolesc. Gynecol.* 34(2), 265 (2021)
- Lall, D., Alexander, D., Maharaj, R., Narace, I., Soroush, M.: Utilization of produced condensate for enhanced oil recovery: a case study for the forest reserve field in trinidad. *J. Petroleum Exploration Prod.* 11(2), 961–972 (2021)
- Cheng, Z., Qin, H., Chen, L., Zhao, X., Yin, S.: Relationship between mining thickness and peak position of advancing abutment pressure: a case study in helin coal mine in china. *Arabian J. Geosci.* 14(12), 1–8 (2021)
- Hoxha, E., Maierhofer, D., Saade, M., Passer, A.: Influence of technical and electrical equipment in life cycle assessments of buildings: case of a laboratory and research building. *Int. J. Life Cycle Assess.* 26(5), 852–863 (2021)
- Zheng, H., Sha, P., Zhai, J., Pan, W., Li, Z., Mi, Z., He, F., Zhang, X., Dai, J., Han, R., Ge, R.: Development and vertical tests of 650 mhz 2-cell superconducting cavities with higher order mode couplers. *Nucl. Instrum. Methods Phys. Res., Sect. A*, 995(1), 165093 (2021)
- Zhang, B., Liu, B., Xing, Y., Carrera, E., & Pagani, A. Free vibration analysis of variable stiffness composite laminated beams and plates by novel hierarchical differential quadrature finite elements. *Compos. Struct.* 274(6), 114364 (2021)
- Hou, P., Ma, H., Ju, P., Chen, X., Zhu, C.: A new vibration analysis approach for monitoring the working condition of a high-voltage shunt reactor. *IEEE Access* 9(99), 1-1 (2021). <https://doi.org/10.1109/ACCESS.2021.3068264>
- Chen, Q., Ma, W., Fei, Q., Devriendt, H., Desmet, W.: An efficient wave based method for the mid-frequency transverse vibration analysis of a thermal beam with interval uncertainties. *Aerosp. Sci. Technol.* 110(8), 106438 (2021).
- Bian, P., Hai, Q.: Torsional static and vibration analysis of functionally graded nanotube with bi-helmholtz kernel based stress-driven nonlocal integral model *. *Appl. Math. Mech.* 42(3), 425–440 (2021)
- Ri, K., Han, W., Pak, C., Kim, K., Yun, C.: Nonlinear forced vibration analysis of the composite shaft-disk system combined the reduced-order model with the ihb method. *Nonlinear Dyn.* 104(4), 3347–3364 (2021)
- Conle, F.A., Mousseau, C.W. Using vehicle dynamics simulations and finite-element results to generate fatigue life contours for chassis components. *Int. J. Fatigue* 13(3), 195–205 (1991).
- Sane, S.S., Jadhav, G., Anandraj, H.: Stress analysis of light commercial vehicle chassis by FEM. //Piaggio Vehicle Pte. Ltd pune. stress analysis of heavy duty truck chassis using finite element method, *Philos. Trans. R. Soc. London*, A247, 529–551 (1955).
- Guo, Y.Q., Chen, W.Q., Pao, Y.H.: Dynamic analysis of space frames: The method of reverberation-ray matrix and the orthogonality of normal modes. *J. Sound Vib.* 317(3–5), 716–738 (2008)
- Kim, V., Lee, V.: Elastic foundation effects on the dynamic response of engine mount systems. *Proc. Inst. Mech. Eng.*, 214(D), 43–53 (2000)
- Kotari, S., Gopinath, V.: Static and dynamic analysis on tatra chassis. *Int. J. Mod. Eng. Res.* 2(1), 086–094 (2002)
- Marzbanrad, J., Alijanpour, M., Saeidkiasat, M.: Design and analysis of an automotive bumper beam in low-speed frontal crashes. *Thin Walled Struct.* 47, 902–911 (2009)

33. Xu, H.J., Liu, Y.Q., Zhong, W.: Three-dimensional finite element simulation of medium thick plate metal forming and springback. *Finite Elem. Anal. Des.* 51, 49–58 (2012)
34. Chakraborty, C., Kishor, A.: Real-time cloud-based patient-centric monitoring using computational health systems. In *IEEE Transactions on Computational Social Systems*, <https://doi.org/10.1109/TCSS.2022.3170375>
35. Kishor, A., Chakraborty, C., Jeberson, W.: Reinforcement learning for medical information processing over heterogeneous networks. *Multimedia Tools Appl.* 80(16), 23983–24004 (2021).
36. Timoshin, A., Kazemi, A., Beni, M.H., Jam, J.E., Pham, B.: Nonlinear strain gradient forced vibration analysis of shear deformable microplates via hermitian finite elements. *Thin Walled Struct.* 161(11), 107515 (2021)
37. Ahmadi, I. Vibration analysis of 2d-functionally graded nanobeams using the nonlocal theory and meshless method. *Eng. Anal. Boundary Elem.* 124(8), 142–154 (2021)
38. Aydinlik, S., Kiris, A., Sumelka, W.: Nonlocal vibration analysis of microstretch plates in the framework of space-fractional mechanics—Theory and validation. *Eur. Phys. J. C Part Fields* 136(2), 1–17 (2021).
39. Tang, H., Dai, H.L.: Nonlinear vibration analysis of CFRP spherical shell panel under hygrothermal effects. *Compos. Struct.* 274(2), 114343 (2021)
40. Qiu, B., Du, B., Huang, C., Chen, W., Wang, B.: The numerical simulation of the flow distribution and flow-induced vibration analysis for intermediate heat exchanger in a pool-type fast breeder reactor. *Prog. Nucl. Energy* 131(2), 103605 (2021)
41. Kohansal-Vajargah, M., Ansari, R.: Quadratic tetrahedral micropolar element for the vibration analysis of three-dimensional micro-structures. *Thin Walled Struct.* 167(10), 108152 (2021)
42. Lee, J.W., Lee, J.Y., Dong, M.L.: Free vibration analysis of axially moving beams using the transfer matrix method. *J. Mech. Sci. Technol.* 35(4), 1369–1376 (2021).
43. Jafarishad, H., Ahmadian, M.T.: Dynamic and vibration analysis of a 3-serial-link micro/nano-manipulator with piezoelectric actuation. *Microsyst. Technol.* 27(3), 703–721 (2021)
44. Gk, A., Ph, B., Ka, C., Dc, A., Yr, A., Hr, A.: Free vibration analysis of functionally graded double-beam system using haar wavelet discretization method. *Eng. Sci. Technol., Int. J.* 24(2), 414–427 (2021).
45. Ponci, L.P., Creci, G., Menezes, J.C.: Simplified procedure for vibration analysis and dynamic balancing in mechanical systems with beats frequency. *Measurement* 174(4), 109056 (2021)
46. Rostamijavanani, A., Ebrahimi, M.R., Jahedi, S.: Free vibration analysis of composite structures using semi-analytical finite strip method. *J. Fail. Anal. Prev.* 21(3), 927–936 (2021)
47. Liu, W., Sun, H.L., Zhao, Q.: Free vibration and transmission response analysis for torsional vibration of circular annular plate. *Iran. J. Sci. Technol.* 45(3), 631–638 (2021).
48. Jafarishad, H., Ahmadian, M.T.: Dynamic and vibration analysis of a 3-serial-link micro/nano-manipulator with piezoelectric actuation. *Microsyst. Technol.* 27(3), 703–721 (2021).
49. Hoxha, E., Maierhofer, D., Saade, M., Passer, A.: Influence of technical and electrical equipment in life cycle assessments of buildings: case of a laboratory and research building. *Int. J. Life Cycle Assess.* 26(5), 852–863 (2021).
50. Zheng, H., Sha, P., Zhai, J., Pan, W., Ge, R.: Development and vertical tests of 650 mhz 2-cell superconducting cavities with higher order mode couplers. *Nucl. Instrum. Methods Phys. Res., Sect. A*, 995(1), 165093 (2021)
51. Banakh, L.Y. Dynamic fractals in biomechanics: the vibration receptors of Pacinian corpuscles. *J. Mach. Manuf. Reliab.* 50(1), 19–25 (2021)

How to cite this article: Wang, D., Dai, L., Zhang, X., Sayyad, S., Sugumar, R., Kumar, K., Asenso, E.: Vibration signal diagnosis and conditional health monitoring of motor used in biomedical applications using Internet of Things environment. *J. Eng.* 1–9 (2022). <https://doi.org/10.1049/tje2.12203>